

## Segregation dynamics of binary mixtures with simple chemical reactions

This article has been downloaded from IOPscience. Please scroll down to see the full text article.

1994 J. Phys. A: Math. Gen. 27 6027

(<http://iopscience.iop.org/0305-4470/27/18/013>)

View [the table of contents for this issue](#), or go to the [journal homepage](#) for more

Download details:

IP Address: 171.66.16.68

The article was downloaded on 01/06/2010 at 23:26

Please note that [terms and conditions apply](#).

## Segregation dynamics of binary mixtures with simple chemical reactions

Sanjay Puri† and H L Frisch‡

† School of Physical Sciences, Jawaharlal Nehru University, New Delhi-110067, India and  
Institut für Physik, Johannes Gutenberg-Universität Mainz, D-55099 Mainz, Germany

‡ Department of Chemistry, SUNY at Albany, Albany, NY 12222, USA

Received 6 January 1994, in final form 17 March 1994

**Abstract.** The dynamics of segregation of a binary mixture AB with chemically active components are studied. For simplicity, the study is confined to chemical reactions in which the reactants and end-products consist of only A or B. A phenomenological model and detailed numerical results for the reaction  $AB \rightleftharpoons BB$  in the specific case when the forward and backward reactions proceed at the same rate are presented.

A classical problem in non-equilibrium statistical mechanics is the study of homogeneous binary mixtures which have suddenly been rendered far-from-equilibrium by (say) a temperature or pressure quench [1]. Much interest has focused on the dynamics whereby such systems approach their final equilibrium state and this area of study is now referred to as ‘phase ordering dynamics’. As is natural, initial investigations have been largely confined to the study of pure, isotropic systems. There is now a complete experimental and numerical understanding of phase ordering dynamics in pure, isotropic two-component mixtures—though there are still many outstanding theoretical questions [1]. It is now well accepted that the temporal evolution of these systems is characterized by the appearance of domains which are rich in either of the two components. These domains are characterized by a unique, time-dependent length scale  $L(t)$  (where  $t$  is time), which has a power-law dependence asymptotic in time, namely  $L(t) \sim t^\phi$ . The growth exponent  $\phi$  depends critically on whether or not the order parameter is conserved. For the case of non-conserved order parameter (e.g. the ordering of a ferromagnet),  $\phi = \frac{1}{2}$ —the so-called Lifshitz–Cahn–Allen law. For the case of conserved order parameter without hydrodynamic effects (e.g. the segregation of a binary alloy),  $\phi = \frac{1}{3}$ , which is known as the Lifshitz–Slyozov growth law. Finally, for the case of conserved order parameter with hydrodynamic effects (e.g. the segregation of binary fluids), it has been known for some time experimentally and has recently been demonstrated numerically [2] that  $\phi = 1$ .

Recently, attention has turned to the problems of phase ordering dynamics in more realistic experimental situations. The aim of such studies is usually two-fold. First, they attempt to formulate a reasonable model which incorporates the relevant ‘experimentally realistic’ effect. Secondly, they study these models numerically and analytically, though the analysis is mostly numerical because of the substantial analytical difficulties involved—even at the level of pure, isotropic systems. To name a few examples, there have been a number of studies of important phenomena, like strain effects in segregating binary alloys [3]; gravitational effects [4]; the role of quenched disorder in slowing down domain growth

[5]; and the effect of a surface with a preferential attraction for one of the components of a binary mixture [6].

In this paper, a study is made of the interplay between chemical reactions and segregation dynamics in quenched binary mixtures AB without hydrodynamic effects. At present, investigations are confined to simple model reactions in which the initial reactants and end products are either A or B, the components of the binary mixture. As illustrated shortly, these simple chemical reactions will have the effect of introducing terms which do not conserve the order parameter into the dynamical equations. The model chemical reactions investigated are as follows:

- (i)  $A \rightleftharpoons B$ ;
- (ii)  $AA \rightleftharpoons BB$ ;
- (iii)  $AB \rightleftharpoons BB$ . This reaction occurs only at domain interfaces in the forward direction.
- (iv)  $AB \text{ or } BA \rightleftharpoons AA \text{ or } BB$ . This reaction occurs only at the domain interfaces.

In reactions (i)–(iii), a time-scale  $1/\tau_1$  is associated with the reaction in the forward direction and a time-scale  $1/\tau_2$  with the reaction in the backward direction. In reaction (iv), time-scales  $1/\tau_1$  and  $1/\tau_2$  are associated with reactions in which the end products are AA and BB, respectively.

Before presenting results from these investigations, it is useful to clarify the oversimplifications associated with the proposed model systems. Real solids are imperfect and diffusive transport, particularly in chemically reactive systems, involves lattice defects. Sometimes, these are point defects such as interstitials, vacancies and impurities. More often, these are extended defects such as dislocations, grain boundaries, etc. The usual Kawasaki spin-exchange dynamics [1] is, at best, an approximate model of atomic motion in such systems. Furthermore, phase transformations are rarely isomorphic and new phases are often formed in the transformation of chemically reactive solid systems [7]. Even when the overall kinetics is described by the simple cases (i)–(iv), the actual mechanism [8] of the reaction is complex, involving many intermediate steps and transient phases not described by a simple lattice-gas model. Thus, there are only a few examples of systems which may be approximated by these overly simplistic models. An example of an irreversible reaction in case (i) is the radioactive dissociation of a radioactive atom A into a daughter atom B which can occupy vacancy sites in the A-lattice. (It is interesting to note that the coarse-grained models obtained for case (i) (not presented here) are identical to those proposed by Oono and Shiwa [9] in the context of the apparently unrelated problem of spinodal decomposition in block copolymers.) The photochemical solid-state dimerization of cinnamonic acid, anthracene and some of their derivatives are possible examples of reactions under case (ii) or limiting cases of (iii) or (iv) [10–12]. The existence of catalytic related disordered isomorphous crystals [13] may also be the product of simple kinetics as in cases (ii)–(iv) although the precise nature of the kinetics of formation of these crystals is still to be well understood.

In this paper, representative results are presented from investigations of these simple models. Specifically, a phenomenological model is formulated for the reaction in (iii) and numerical results provided from simulations of this model. Detailed modelling and numerical results for all the reactions mentioned above will be presented later.

A binary mixture (with components A and B) is considered which has been quenched below its bulk critical temperature  $T_c$ . The dynamics of this mixture is conveniently described in the context of an Ising model with a spin variable  $S_i$  at site  $i$ . If the spin variable takes the value  $+1$  ( $-1$ ) at a site, we say that the site is occupied by an A-atom (B-atom). There are two ingredients in the dynamics. First, there is the drive of the

system to segregate into A-rich and B-rich domains. This is successfully described at the microscopic level by spin-exchange or Kawasaki dynamics and at the phenomenological level by the Cahn–Hilliard equation [14, 6], namely

$$2\tau_s \frac{\partial \phi}{\partial \tau}(\mathbf{x}, \tau) = -a^2 \nabla^2 \left\{ \left( \frac{T_c}{T} - 1 \right) \phi(\mathbf{x}, \tau) - \frac{1}{3} \phi(\mathbf{x}, \tau)^3 + \frac{T_c}{qT} a^2 \nabla^2 \phi(\mathbf{x}, \tau) \right\} \quad (1a)$$

where  $\tau_s$  is the characteristic time for a spin-exchange process;  $a$  is the lattice spacing; and  $\phi(\mathbf{x}, \tau)$  is the order parameter at point  $\mathbf{x}$  and time  $\tau$ . In (1a),  $T$  is the temperature and  $q$  is the coordination number of each site on the Ising lattice. Equation (1a) can be put in a dimensionless form by introducing the rescaled variables

$$\psi = \sqrt{\frac{T}{3(T_c - T)}} \phi \quad r = \frac{\mathbf{x}}{a} \sqrt{\frac{q(T_c - T)}{T_c}} \quad t = \frac{\tau}{2\tau_s} \frac{q(T_c - T)^2}{T_c T}.$$

The resultant dimensionless Cahn–Hilliard equation is

$$\frac{\partial \psi}{\partial t}(\mathbf{r}, t) = -\nabla^2 \{ \psi(\mathbf{r}, t) - \psi(\mathbf{r}, t)^3 + \nabla^2 \psi(\mathbf{r}, t) \} \quad (1b)$$

where  $\psi(\mathbf{r}, t)$  is the order parameter at (dimensionless) point  $\mathbf{r}$  and time  $t$ . The dynamics of (1b) is such that an initially disordered system segregates into domains with  $\psi = \pm 1$  in the bulk. The second ingredient in the dynamics is the chemical reaction which we are interested in. To obtain a coarse-grained description of the effect of this reaction, a master equation description is invoked as follows:

$$\begin{aligned} \frac{\partial P}{\partial t}(\{S_1, \dots, S_i, \dots, S_N\}, t) = & - \sum_i W(S_i \rightarrow -S_i) P(\{S_1, \dots, S_i, \dots, S_N\}, t) \\ & + \sum_i W(-S_i \rightarrow S_i) P(\{S_1, \dots, -S_i, \dots, S_N\}, t). \end{aligned} \quad (2)$$

Equation (2) describes the evolution of the time-dependent probability distribution function for  $N$  spins, namely  $P(\{S_1, \dots, S_i, \dots, S_N\}, t)$ . For simplicity, it is assumed that the spins are arranged on a simple cubic lattice. The first term on the right-hand side corresponds to the probability of a spin  $S_i$  flipping to  $-S_i$  with all other spins remaining unchanged, i.e. escape from the configuration  $\{S_1, \dots, S_i, \dots, S_N\}$ . The second term on the right-hand side corresponds to the probability of a spin  $-S_i$  flipping to  $S_i$  with all other spins remaining unchanged, i.e. contributions to the configuration considered. The crucial information is in the transition probabilities  $W(S_i \rightarrow -S_i)$ . Recall that the reaction of interest here is



so that A (or B) is converted to B (or A) only in the presence of an atom of B. Bulk regions of A do not undergo any change in this reaction. The transition probabilities which describe this reaction are

$$W(S_i \rightarrow -S_i) = \frac{1}{\tau_1} \delta_{S_i, 1} \sum_l \delta_{S_l, -1} + \frac{1}{\tau_2} \delta_{S_i, -1} \sum_l \delta_{S_l, 1} \quad (4)$$

where  $l_i$  refers to the neighbours of  $i$ .  $W(-S_i \rightarrow S_i)$  is obtained by replacing  $S_i$  with  $-S_i$  on the right-hand side of (4). If we replace (4) in (2), multiply both sides by the spin-variable  $S_k$  and average over all configurations, we obtain (using  $S_k^2 = 1$ )

$$\frac{\partial}{\partial t} \langle S_k \rangle = -\frac{1}{2\tau_1} \sum_{l_k} \langle (S_k + 1)(1 - S_{l_k}) \rangle - \frac{1}{2\tau_2} \sum_{l_k} \langle (S_k - 1)(1 - S_{l_k}) \rangle \quad (5)$$

where the angular brackets denote the configuration averaging. So far, there have been no approximations. We proceed to a continuum description by using a mean-field decoupling approximation and identifying  $\langle S_k \rangle = \phi(x, \tau)$ , where  $x$  and  $\tau$  are not dimensionless variables as yet. Finally, we Taylor expand the order parameter at the neighbouring sites [15] and obtain the following coarse-grained equation:

$$\begin{aligned} \frac{\partial \phi}{\partial \tau}(x, \tau) = & \frac{-q}{2\tau_1} [1 - \phi(x, \tau)^2] + \frac{q}{2\tau_2} [1 - \phi(x, \tau)]^2 \\ & + \frac{a^2}{2} \left( \frac{1}{\tau_1} - \frac{1}{\tau_2} \right) \nabla_x^2 \phi(x, \tau) + \frac{a^2}{2} \left( \frac{1}{\tau_1} + \frac{1}{\tau_2} \right) \phi(x, \tau) \nabla_x^2 \phi(x, \tau). \end{aligned} \quad (6)$$

In (6),  $q$  is the coordination number of the lattice;  $a$  is the lattice spacing; and we have only retained derivatives up to second order. Because of the approximations involved, equation (6) should be treated as a phenomenological equation. To ascertain its reasonableness, we can consider various limiting cases as follows:

(a) When  $1/\tau_1 \neq 0$  and  $1/\tau_2 = 0$  (only forward reaction), we have the homogeneous fixed points  $\phi^* = +1, -1$ . The first one corresponds to unstable equilibrium (all A's) and the second one corresponds to stable equilibrium (all B's).

(b) When  $1/\tau_1 = 0$  and  $1/\tau_2 \neq 0$  (only backward reaction), we have only one homogeneous fixed point  $\phi^* = 1$ , which corresponds to stable equilibrium (all A's).

(c) When  $1/\tau_1 = 1/\tau_2 = a'$ , we have the equation

$$\frac{\partial \phi}{\partial \tau}(x, \tau) = -\alpha' q \phi(x, \tau)(1 - \phi(x, \tau)) + \alpha' a^2 \phi(x, \tau) \nabla_x^2 \phi(x, \tau). \quad (7)$$

Equation (7) has the homogeneous fixed points  $\phi^* = +1$  (unstable equilibrium, all A's) and  $\phi^* = 0$  (stable equilibrium, homogeneous mixture).

In this paper, we focus on case (c) above. If we use the same rescaling that renders the Cahn-Hilliard equation dimensionless, we find that at a particular temperature ( $T = 0.75T_c$ ), equation (7) has the particularly simple dimensionless form

$$\frac{\partial \psi}{\partial t}(\mathbf{r}, t) = -\alpha \psi(\mathbf{r}, t)(1 - \psi(\mathbf{r}, t)) + \frac{\alpha}{\psi} \psi(\mathbf{r}, t) \nabla^2 \psi(\mathbf{r}, t) \quad (8)$$

where  $\alpha$  is a phenomenological constant ( $\alpha = 24\tau_s \alpha'$ , where  $\tau_s$  is the characteristic time for a spin-exchange). Thus, the equation for the segregation of a binary mixture whose components are undergoing the specified chemical reaction is as follows:

$$\begin{aligned} \frac{\partial \psi}{\partial t}(\mathbf{r}, t) = & -\nabla^2 \{ \psi(\mathbf{r}, t) - \psi(\mathbf{r}, t)^3 + \nabla^2 \psi(\mathbf{r}, t) \} \\ & - \alpha \psi(\mathbf{r}, t)(1 - \psi(\mathbf{r}, t)) + \frac{\alpha}{\psi} \psi(\mathbf{r}, t) \nabla^2 \psi(\mathbf{r}, t). \end{aligned} \quad (9)$$

To obtain (9), the terms on the right-hand side of (1b) and (8) have simply been added, as the segregation dynamics do not interfere with the reaction dynamics. Notice that (9) does not conserve the order parameter. The constant  $\alpha$  fixes the relative time-scales of segregation and the chemical reaction. The homogeneous solution  $\psi^* = 0$  ( $\psi^* = 1$ ) is unstable (stable) for the segregation dynamics but stable (unstable) for the chemical reaction. For the important case of fluctuations around a zero background (i.e. the critical quench), a simple analysis shows that the fluctuations grow if  $\alpha < \frac{1}{4}$ . Our results show that the system evolves into interesting microstructures which depend critically on the relative time-scales of segregation and the chemical reaction.

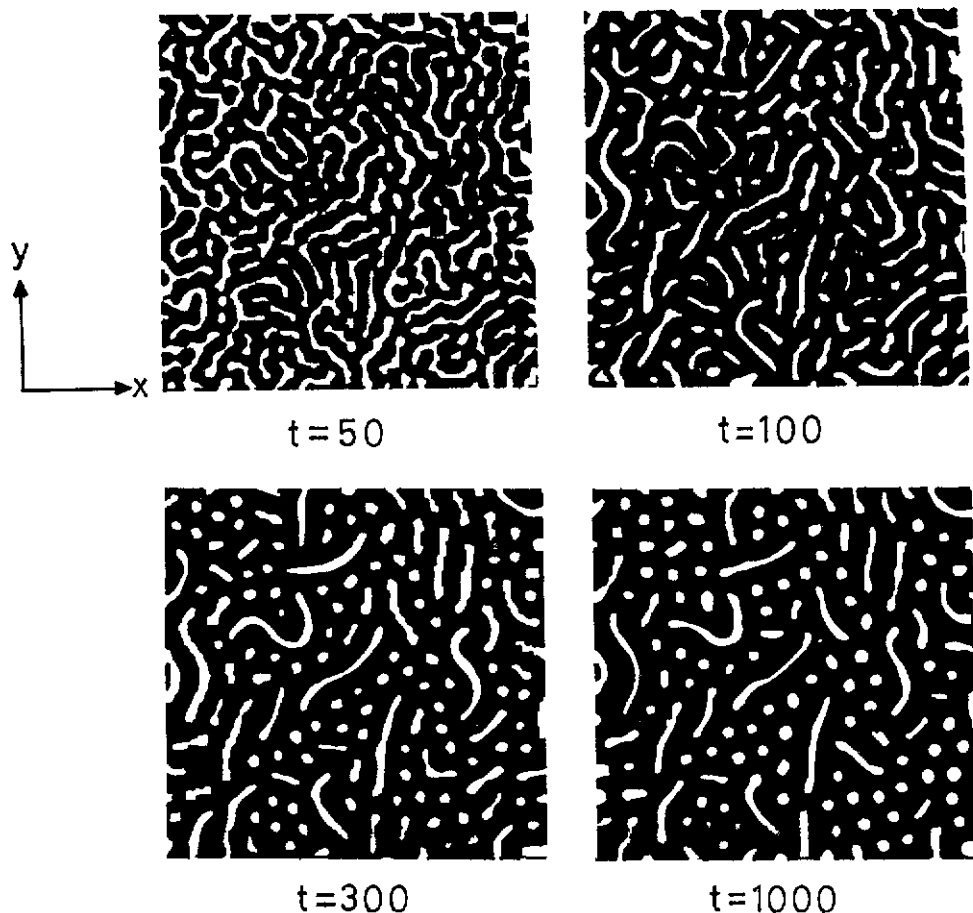
We have numerically simulated equation (9) using a simple Euler discretization on two-dimensional lattices of size  $N_x \times N_y$  (where  $N_x = N_y = 256$ ) with periodic boundary conditions. The discretization mesh sizes are  $\Delta t = 0.1$  and  $\Delta x = 1.7$ . These mesh sizes are too coarse to give a numerical solution which accurately shadows the solution of the original partial differential equation. Rather, this discrete model should be understood in the spirit of cell dynamical system (CDS) models [16]. Simulations reported here are for the parameter value  $\alpha = 0.01$ . We will describe the different microstructures the system evolves into for different values of  $\alpha$  elsewhere. In these simulations, the initial conditions always consisted of uniformly distributed random fluctuations of amplitude 0.05 about a zero background, i.e. the so-called critical quench.

Figure 1 shows evolution pictures for the discrete model from early times to times where it freezes into a microstructure. Sites with positive order parameter (i.e. rich in A) are marked black. The early time patterns are reminiscent of the bicontinuous structure of spinodal decomposition. However, this structure soon breaks up into a mixture of spherical domains and worm-like domains of the B-rich phase in a background of the A-rich phase. For times  $t > 1000$ , there is no further evolution of the system and it is frozen into the microstructure shown for  $t = 1000$ . Figure 2 shows the evolution of order-parameter profiles along a cross section at  $y = L/2$  (where  $L = N_y \Delta x$ ) for the snapshots of figure 1. As is evident from figures 1 and 2, the system evolves into an off-critical state where A becomes a majority phase and B a minority phase. Figure 3 shows the time dependence of the average order parameter of the system  $\langle \psi \rangle(t)$ , which is a measure of the off-criticality. This quantity rapidly (by about  $t = 200$ ) saturates to its maximum value and remains unchanged after that.

The most remarkable feature of phase ordering dynamics in chemically inert systems is the dynamical scaling of the time-dependent structure factor [17], namely

$$S(\mathbf{k}, t) = \langle \psi(\mathbf{k}, t) \psi(\mathbf{k}, t)^* \rangle \quad (10)$$

where the angular brackets denote an averaging over initial conditions; and  $\psi(\mathbf{k}, t)$  is the Fourier transform of  $\psi(\mathbf{r}, t)$ . Dynamical scaling is a consequence of the existence of a unique characteristic length scale  $L(t)$  and  $F(x)$  is a universal function, which is time-independent and reflects the morphology of domain growth. In our chemically active system, the morphology evolves continuously in time and the structure factor would not be expected to scale dynamically. This is confirmed in figure 4(a), where we superpose data for  $S(\mathbf{k}, t) \langle k \rangle^2$  versus  $k/\langle k \rangle$  from times  $t = 100, 300$  and  $1000$ , where  $\langle k \rangle$  is the first moment of the structure factor and is a measure of the reciprocal of the characteristic length scale, if it exists [16]. (The structure-factor data in figure 4(a) has been obtained as an average over 100 independent initial conditions and after spherically averaging the vector function  $S(\mathbf{k}, t)$ .) Furthermore, inspecting the evolution pictures at  $t = 1000$ , one might be tempted to speculate that the morphology of this system may be related to that



**Figure 1.** Evolution pictures obtained from an Euler-discretized version of the model (equation (9)) for the segregation dynamics of a binary mixture AB undergoing the simple chemical reaction described in the text. The discretization mesh sizes are  $\Delta t = 0.1$  and  $\Delta x = 1.7$  and the lattice size is  $N_x \times N_y$ , where  $N_x = N_y = 256$ . Periodic boundary conditions are applied in both directions. The initial condition consists of uniformly distributed random fluctuations of amplitude 0.05 about a background of zero, i.e. the so-called critical quench. Regions with positive order parameter (A-rich) are marked in black. Pictures are shown for dimensionless times  $t = 50, 100, 300$  and  $1000$ .

for segregation dynamics (with no reaction) for an appropriately off-critical quench. This is also not true. Figure 4(b) superposes data for  $S(k, t)/(k)^2$  versus  $k/(k)$  for the evolution described above at  $t = 1000$  and for the Cahn–Hilliard evolution of an off-critical quench (with an average order parameter of 0.38) at  $t = 4000$ . There is obviously no similarity between the two scaled functions.

Finally, we investigate whether the domain-size distributions of the different phases A and B can be individually characterized by unique length scales. For this, we consider the time-dependent domain-size distribution functions  $n_A(L, t)$  and  $n_B(L, t)$ , where  $L$  is the linear domain size. Numerically, these are obtained as follows. For a single run, the order parameter profiles along horizontal and vertical cross sections at all values of  $x$  and  $y$  for the discrete lattice are considered. Each order-parameter profile is numerically examined to

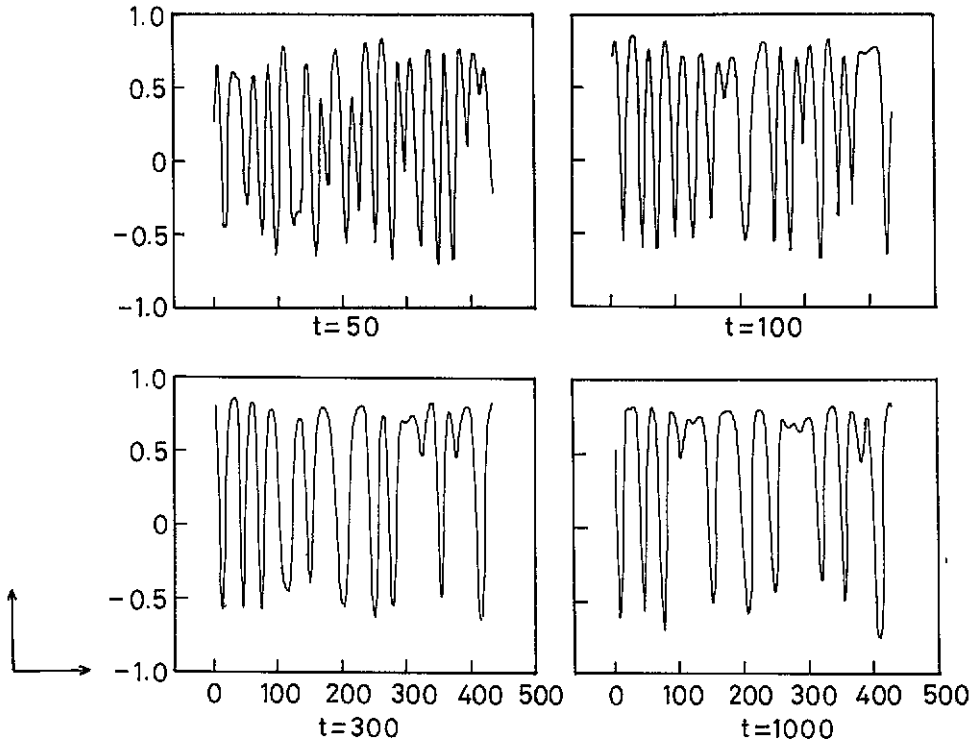


Figure 2. Variation of order parameter for the evolution pictures of figure 1 along a cross section at  $y = L/2$ , where  $L = N_y \Delta x$ . The figure plots  $\psi(x, L/2, t)$  versus  $x$  for the same dimensionless times as in figure 1.

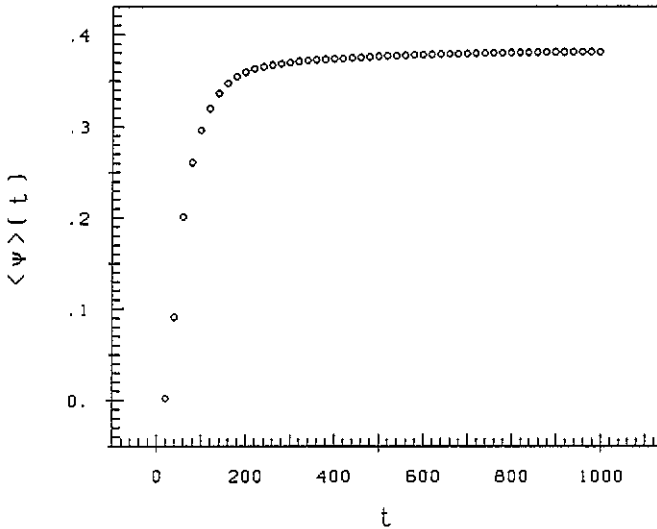
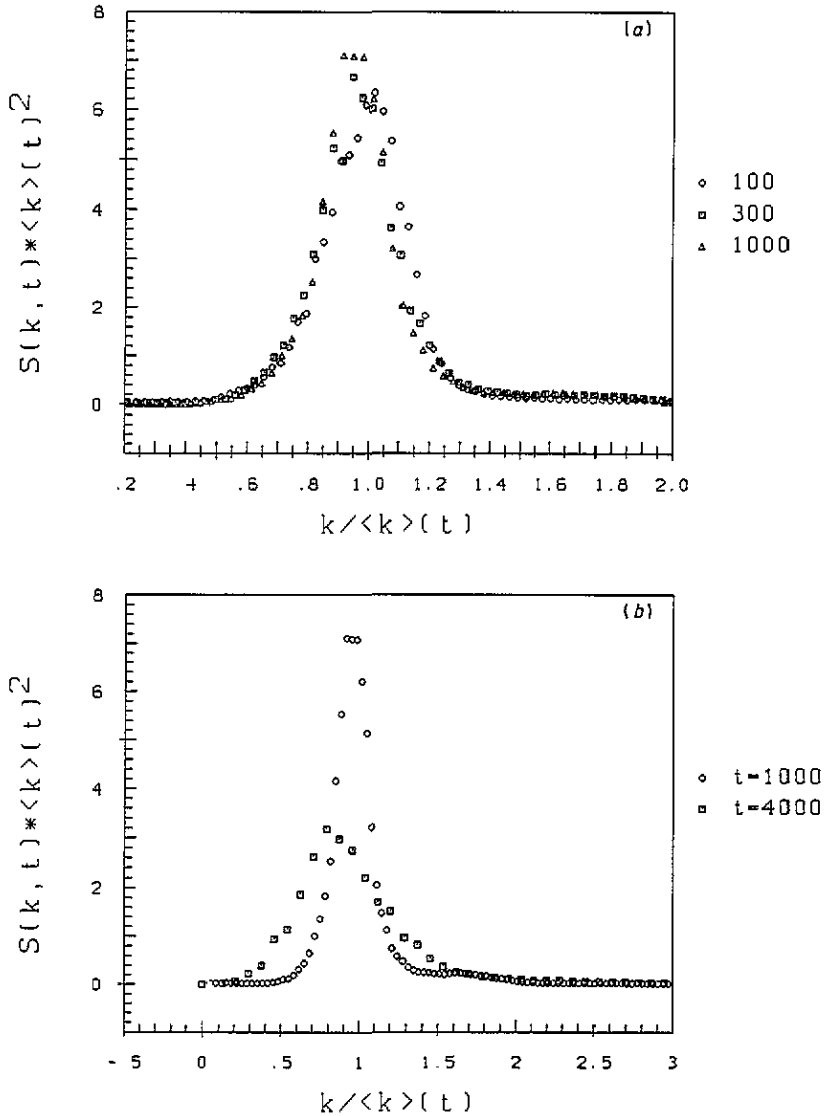


Figure 3. Average order parameter  $\langle \psi \rangle(t)$  as a function of time  $t$  for the evolution shown in figure 1.





**Figure 4.** (a) Plot of  $S(k, t)\langle k \rangle(t)^2$  versus  $k/\langle k \rangle(t)$  from our discrete model for dimensionless times  $t = 100, 300$  and  $1000$  (denoted by the symbols indicated). The time-dependent structure factor  $S(k, t)$  is obtained as an average over 100 independent runs and a spherical averaging of the vector function  $S(k, t)$ . The first moment of  $S(k, t)$  (denoted as  $\langle k \rangle$ ) is taken as a measure of the inverse of the characteristic length scale. (b) Superposition of data for  $S(k, t)\langle k \rangle(t)^2$  versus  $k/\langle k \rangle(t)$  from the discrete model (at time  $t = 1000$ , denoted by circles) and from the evolution of an off-critical quench with  $\langle \psi \rangle = 0.38$  for an Euler-discretized version of the Cahn-Hilliard equation (at time  $t = 4000$ , denoted by squares). The simulation of the Cahn-Hilliard equation was done using the same mesh sizes and system size as described in figure 1. The corresponding structure factor was obtained as an average over 100 independent initial conditions.

determine the location and number of zero crossings, i.e. when the order parameter changes sign. These zero crossings are used to determine the domain-size distributions (for A and B) corresponding to the order-parameter profile. This data is averaged (for each run) over

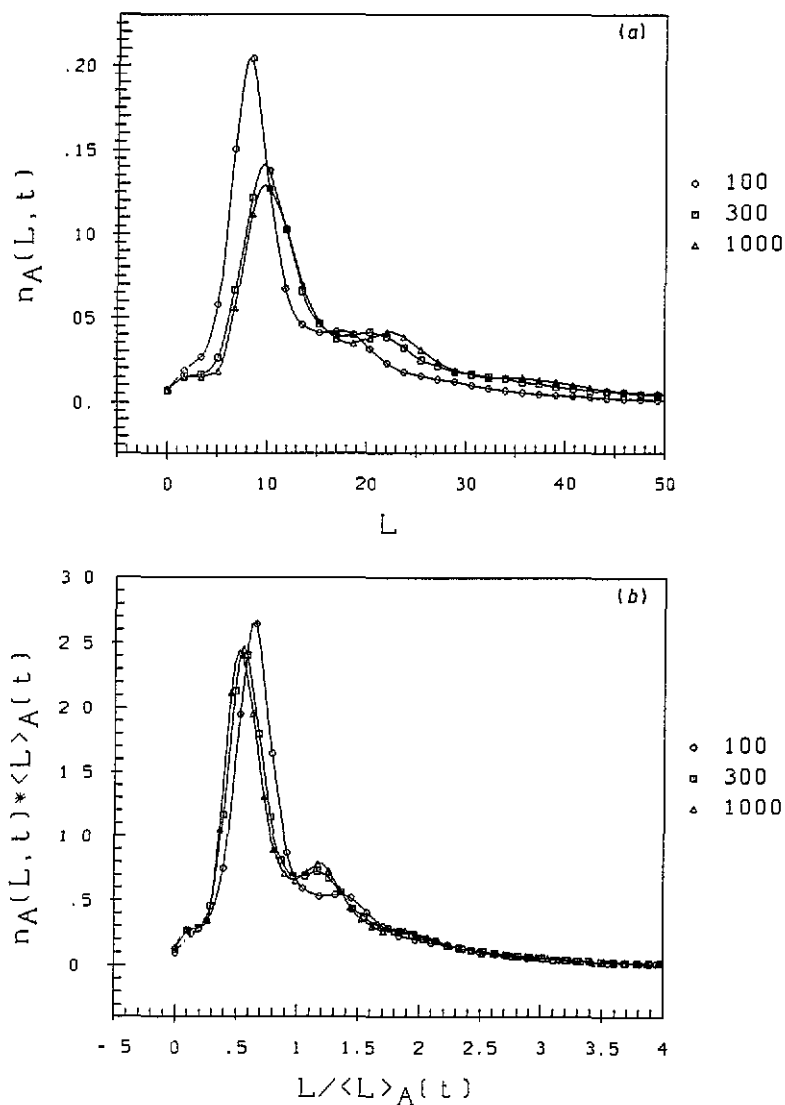


**Figure 5.** (a) Domain-size distribution function for A-rich domains,  $n_A(L, t)$ , as a function of linear domain size  $L$  for dimensionless times  $t = 100, 300$  and  $1000$  (denoted by the indicated symbols). The domain-size distribution function is obtained as an average over 200 independent runs, with averaging over horizontal and vertical sweeps of the lattice for each run. It is normalized to unity. (b) Test of dynamical scaling for the data for  $n_A(L, t)$  from figure 5(a). This figure superposes data for  $n_A(L, t) \langle L \rangle_A(t)$  versus  $L / \langle L \rangle_A(t)$  from dimensionless times  $t = 100, 300$  and  $1000$ , where  $\langle L \rangle_A$  is the first moment of  $n_A(L, t)$ .

the different cross sections (numbering  $N_x \times N_y$  in all) to obtain the domain-size distribution corresponding to a single run. Finally, the domain-size distributions are averaged over 200 independent runs and normalized so that

$$\sum_L n_{A,B}(L, t) = 1$$

where  $L$  takes the discrete values  $n_x \Delta x$ , with  $n_x$  going from 1 to 256. Figure 5(a) plots

the domain-size distribution function for A-rich domains,  $n_A(L, t)$ , as a function of domain size  $L$  for  $t = 100, 300$  and  $1000$ . The distinctive feature of the distribution at later times is the development of a subsidiary peak. If this distribution is characterized by a single length  $L_A(t)$ , it should exhibit the dynamical scaling form  $n_A(L, t) = (L_A(t))^{-1} f(L/L_A(t))$ , where  $f(x)$  is independent of time. Figure 5(b) plots  $n_A(L, t)\langle L \rangle_A$  versus  $L/\langle L \rangle_A$  for  $t = 100, 300$  and  $1000$ , where the first moment of the domain-size distribution function (denoted by  $\langle L \rangle_A$ ) has been taken as a measure of the characteristic length scale. The data collapse is not good through the entire range of times, suggesting that the domain-size distribution function for A-rich domains does not scale dynamically. (Similar results are obtained if the position of the higher peak of the distribution function is used as a measure of the characteristic length scale. The results are not shown here.)

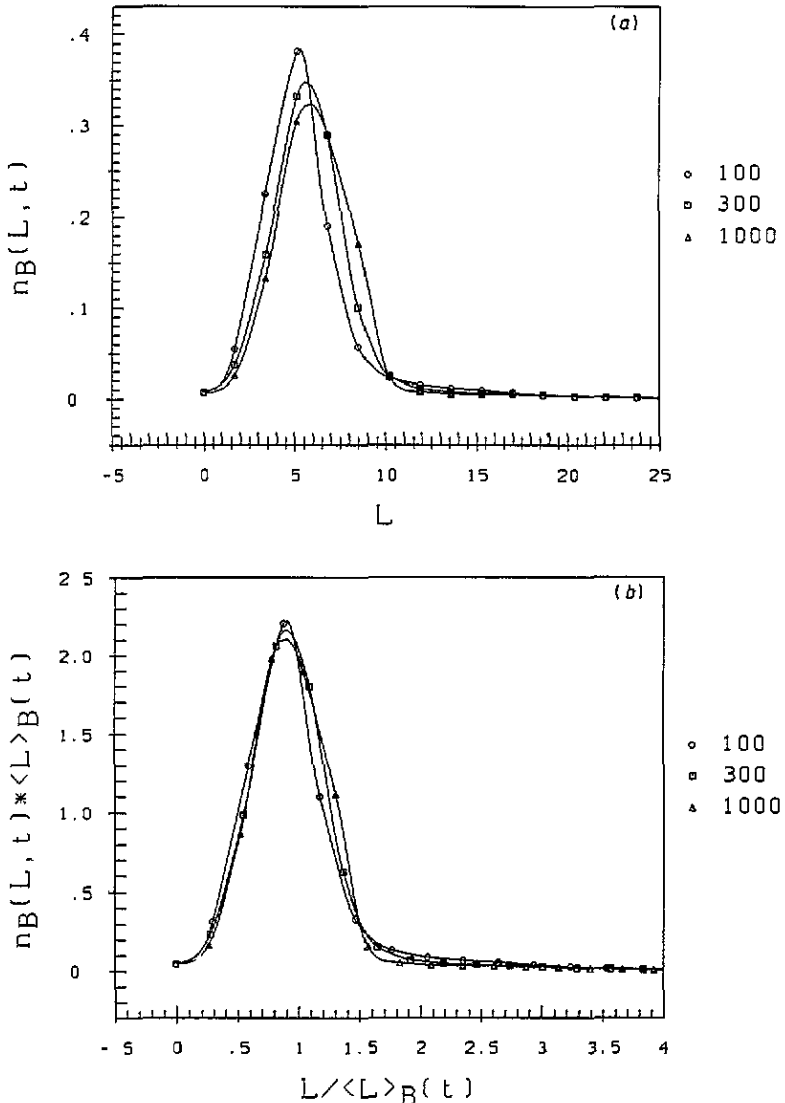


Figure 6. (a) Analogous to figure 5(a), and (b) analogous to figure 5(b), but for the B-rich domains.

Figure 6(a) plots the domain-size distribution function for B-rich domains  $n_B(L, t)$ , as a function of domain size  $L$  for times  $t = 100, 300$  and  $1000$ . Figure 6(b) investigates the dynamical scaling of  $n_B(L, t)$ , again using its first moment  $\langle L \rangle_B$  as a measure of the characteristic domain size. Once again, the data collapse is not good, though it is somewhat better than in figure 5(b). Of course, one should keep in mind that  $n_B(L, t)$  has a much weaker time dependence than  $n_A(L, t)$  and this is responsible for the deceptively better dynamical scaling in figure 6(b).

For completeness, we plot the time dependence of the first moments of the domain-size distribution functions for A-rich and B-rich domains in figure 7. The average size of A-rich domains saturates out to a much larger value than that for B-rich domains, but there is little growth in either for  $t > 400$ .

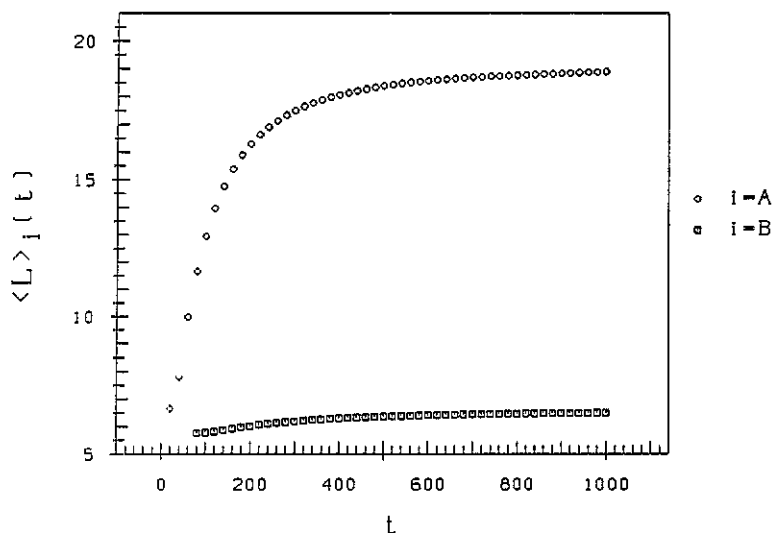


Figure 7. Time dependence of the first moments  $\langle L \rangle_A$  and  $\langle L \rangle_B$  of the domain-size distribution functions for the A-rich and B-rich domains, respectively.

Let us end with a brief summary and discussion of these results. The dynamics of segregation of binary mixtures of chemically active components A and B have been modelled. At present, this has been confined (for simplicity) to reactions in which the initial reactants and end products are either A or B. The effect of these reactions is to introduce non-conserving terms into the segregation dynamics, which is usually described by the order-parameter conserving Cahn–Hilliard equation. The effects of these reactions are easily modelled by using an approach based on the master equation. These results indicate that the evolution morphology of such a system depends critically on the relative time-scales of segregation and the chemical reaction. In this paper, a model for the reversible reaction  $AB \rightleftharpoons BB$  has been presented and detailed numerical results given for the case in which the forward and backward reactions proceed at the same rate. Our results indicate that there are multiple length scales characterizing the evolution dynamics. The time-dependent structure factor does not exhibit dynamical scaling and neither do the individual domain-size distribution functions.

This paper is the first part of a larger study where we intend to study general reactions of the type  $A + B \rightleftharpoons C + D$ , where C may or may not be the same as D. Naturally, the

presence of components other than A or B complicates the problem considerably as it renders incomplete even the Cahn–Hilliard description of segregation dynamics. A complete model can be motivated from a master equation approach to spin- $n$  models, where the total number of components involved as both reactants and end products is  $2n + 1$  [18]. Conceptually, this poses no problems but the partial differential equations that result are considerably more complicated.

## Acknowledgments

SP is grateful to K Binder for his warm hospitality at Mainz, where part of the work described in the text was carried out. SP is also grateful to the Deutsche Forschungsgemeinschaft (DFG) for supporting his stay at Mainz under Sonderforschungsbereich 262. The authors are also supported, in part, by National Science Foundation grant DMR 9023541.

## References

- [1] For reviews see, Gunton J D, San Miguel M and Sahni P S 1983 *Phase Transitions and Critical Phenomena* vol 8, ed C Domb and J L Lebowitz (New York: Academic) p 267  
Furukawa H 1885 *Adv. Phys.* **34** 703  
Binder K 1991 *Phase Transformations of Materials (Materials Science and Technology 5)* ed P Haasen (Weinheim: VCH) p 405
- [2] Koga T and Kawasaki K 1991 *Phys. Rev. A* **44** R817  
Puri S and Dunweg B 1992 *Phys. Rev. A* **45** R6977  
Stinozaki A and Oono Y 1993 *Phys. Rev. E* **48** 2622
- [3] Onuki A 1989 *J. Phys. Soc. Japan* **58** 3065, 3069  
Nishimori H and Onuki A 1990 *Phys. Rev. B* **42** 980  
Onuki A and Nishimori H 1991 *Phys. Rev. B* **43** 13649
- [4] Kitahara K, Oono Y and Jasnow D 1988 *Mod. Phys. Lett. B* **2** 765  
Puri S, Binder K and Dattagupta S 1992 *Phys. Rev. B* **46** 98  
Yeung C, Rogers T, Machado A H and Jasnow D 1992 *J. Stat. Phys.* **548** 1141
- [5] Puri S, Chowdhury D and Parekh N 1991 *J. Phys. A: Math. Gen.* **24** L1087  
Puri S and Parekh N 1993 *J. Phys. A: Math. Gen.* **26** 2777  
Bray A J and Humayun K 1991 *J. Phys. A: Math. Gen.* **24** L1185
- [6] Binder K and Frisch H L 1991 *Z. Phys. B* **84** 403  
Puri S and Binder K 1992 *Phys. Rev. A* **46** R4487
- [7] Hannay N B (ed) 1976 *Treatise on Solid State Chemistry* vol 4 (New York: Plenum)
- [8] Moore J W and Pearson R G 1981 *Kinetics and Mechanism* 3rd edn (New York: Wiley)
- [9] Oono Y and Shiwa Y 1987 *Mod. Phys. Lett. B* **1** 49
- [10] Jacobs P W 1969 *Proc. Sixth Int. Symp. on the Reactivity of Solids* ed J W Mitchell *et al* (New York: Wiley) p 207
- [11] Thomas J M and Williams J O 1971 *Progress in Solid State Chemistry* vol 6, ed H Reiss and J O McCaldin (Oxford: Pergamon) p 119
- [12] Cohen M D and Schmidt G M J 1964 *J. Chem. Soc.* 1996  
Cohen M D, Schmidt G M J and Sonntag F I 1964 *J. Chem. Soc.* 2000
- [13] Place H and Willett R D 1987 *Acta Crystallogr. C* **43** 1497
- [14] Cahn J W 1961 *Acta Metall.* **9** 795 and references therein
- [15] Binder K 1974 *Z. Phys. B* **267** 313 (see also Binder K and Frisch H L [6])
- [16] Oono Y and Puri S 1987 *Phys. Rev. Lett.* **58** 836; 1988 *Phys. Rev. A* **38** 434  
Puri S and Oono Y 1988 *Phys. Rev. A* **38** 1542
- [17] Binder K and Stauffer D 1974 *Phys. Rev. Lett.* **33** 1006; 1976 *Z. Phys. B* **24** 407
- [18] Puri S and Binder K unpublished